Draft version September 26, 2018
Typeset using LaTeX **twocolumn** style in AASTeX62

The Hierarchical Assembly of the Galactic Halo: the Origin of CEMP-no Groups in the Milky Way

Jinmi Yoon,[1] Devin Whitten,[1] Di Tian,[2] Timothy C. Beers,[1] Young Sun Lee,[3] and Vinicius M. Placco[1]

[1]*Department of Physics and JINA-CEE, University of Notre Dame, Notre Dame, IN 46556*
[2]*Department of Physics, Xi'an Jiaotong University, Shaanxi, 710049, People's Republic of China*
[3]*Department of Astronomy and Space Science, Chungnam National University, Daejeon 34134, Korea*

ABSTRACT

Nature hid the first generation of stars and yet left their imprints onto so-called CEMP-no stars. Recently, there have been some doubts about the latest finding that the halo CEMP-no stars can be subdivided into the Group II and Group III stars based on the relation of absolute abundance and metallicity and this bifurcation indicates at least two different pathways to form the CEMP-no stars. In this work, we confirm ~~that~~ the bifurcation of the halo CEMP-no stars ~~truly exists~~ by showing that the CEMP stars from the satellite galaxies also present the similar two groups. Furthermore, we discovered the first Group III CEMP-no star in an ultra-faint dwarf galaxy (UFD), Canes Venatici I. These two important results provide ~~a~~ strong evidence that the halo CEMP-no stars were accreted into the Galactic halo. More interestingly, we also found that only CEMP stars from the UFDs have both Group II and Group III CEMP-no stars, whereas more massive classical dwarf galaxies (dSph) seem to have only Group II stars. From this finding, we conclude that the understanding the origin of the CEMP-no stars in the halo requires understanding of not only nucleosynthetic processes but also the mass of the host galaxies of these CEMP-no stars, which dilutes stellar elemental yields from the first stars.

Keywords: Galaxy: halo - galaxies: dwarf - galaxies: individual (CVn I) - stars: abundances - stars: chemically peculiar - stars: individual (SDSS J132755.56+333521.7) - stars: Population II

1. INTRODUCTION

One of the primary goals in Galactic Archaeology, a study of ancient stars, is understanding the nature of the first stars and their contribution to the chemical enrichment and the Galactic formation in the early Universe. However, the first stars are thought to live for a brief lifetime, explode, and enrich their surrounding pristine gas. Their nucleosynthetic products were locked up in the next-generation stars, through which we are ~~only~~ able to indirectly understand the first stars. The endeavor to find the stellar fossils has led to discovering numerous metal-poor stars (i.e., Beers & Christlieb 2005; Frebel & Norris 2015, and the references therein). Thanks to the efforts, it is widely accepted that the frequency of a chemically peculiar stellar population, so-called carbon-enhanced metal-poor (CEMP[1], Beers & Christlieb 2005; Aoki et al. 2007) stars increases with decreasing metallicity and reaches to unity at metallicity, [Fe/H]$\lesssim -4.0$ (e.g., Lee et al. 2013; Placco et al. 2014; Yoon et al. 2018). Thus the discovery of CEMP stars in the Galactic halo has been crucial for understanding the nearly pristine chemical and physical environment in the early Galaxy. However, not all CEMP subclasses are the direct decedents of the first stars. Only CEMP-no stars, which show peculiarly enhanced abundance patterns of only light elements (C, N, O, and/or Na and Mg) but heavy neutron-capture elements (i.e., Ba and Eu), are thought to be the bonafide second-

Corresponding author: Jinmi Yoon
jinmi.yoon@nd.edu

[1] There are several CEMP sub-classes depending on enhancement of heavy neutron-capture elements such as Ba and Eu. CEMP-*s* : [C/Fe] $\geq +0.7$, [Ba/Fe] $> +1.0$, and [Ba/Eu] $> +0.5$ CEMP-*r* : [C/Fe] $\geq +0.7$ and [Eu/Fe]$> +1.0$ CEMP-*r*/*s* or CEMP-*i* : [C/Fe] $\geq +0.7$ and $0.0 <$ [Ba/Eu] $< +0.5$ CEMP-no : [C/Fe] $\geq +0.7$ and [Ba/Fe] < 0.0. Here we adopt relative abundance ratio as [A/B]$=$ log $(N_A/N_B)_\star$ - log $(N_A/N_B)_\odot$ where N_A and N_B are numbers of elements A and B respectively.

generation of stars formed out of the first-star nucleosynthetic products from faint supernovae (SNe) of massive stars, slow neutron-capture process in rapidly rotating massive stars called as spinstars, and/or intermediate neutron-capture process in massive first-generation stars, based on the various studies (i.e., Meynet et al. 2010; Nomoto et al. 2013; Hansen et al. 2016; Yoon et al. 2016; Placco et al. 2016; Choplin et al. 2017; Clarkson et al. 2018, and the references therein). Their abundance patterns, which are conventionally employed by relative elemental abundance ratios to iron, are more or less well-matched by the aforementioned nucleosynthetic models, especially faint supernova models, ~~even~~ though their fits are not perfect.

The latest challenge in understanding the halo CEMP-no stars emerged when Yoon et al. (2016) claimed the existence of at least two distinct groups among the halo CEMP stars in the space of absolute carbon abundance, A(C)[2] as a function of metallicity. They claimed that multiple progenitors are responsible for the apparent CEMP-no groups. The Group I CEMP stars with the highest A(C) values~~,~~ are predominantly CEMP-s stars whose carbon and barium abundances are enhanced due to the mass-transfer from their companion during its asymptotic branch phase. Although the dominant discussion in the Group I region was about the CEMP-s stars in Yoon et al., we emphasize that a substantial fraction ($\sim$13%) of the CEMP-no stars reside in this region, whose origin is not clear yet (Yoon et al. 2016) and they are worthy of attention in this work. They could be associated with binary mass-transfer origin, however, most of them have still unknown binary status except two binary and two single CEMP-no stars in that region. The Group II and III regions with lower A(C) consist of mainly CEMP-no stars. The Group II CEMP-no stars ($-5.0 \lesssim$ [Fe/H] $\lesssim -3.0$ and $5.0 \lesssim A(\mathrm{C}) \lesssim 7.0$) have its A(C) tracking with [Fe/H], while the Group III CEMP-no stars ([Fe/H]$\lesssim -4.0$ and scatter around $A(\mathrm{C}) \sim 7.0$) have no strong dependency of A(C) on its metallicity, with 1-2 dex higher A(C) than that of the Group II stars. These Group II and III stars also show distinctly different trends found in absolute abundances of Na and Mg as a function of A(C). A few studies have explored to answer the origin of the distinct groups, i.e., different dust grain cooling channels on low-mass star formation (Chiaki et al. 2017) and inhomogenous metal-mixing during bursty star formation (Sharma et al. 2018). However, there are also some doubts about the existence of this complex morphology among the CEMP stars, claiming that the Group II stars are simply a continuation of carbon-normal stars and there is no such birfucated groups among the CEMP-no stars, but only one population (e.g., Spite et al. 2018; François et al. 2018).

Do the multiple groups of the halo CEMP-no stars truly exist? If then, what does ~~the~~ nature tell us about these different groups regarding their formation history? Are different dust cooling and/or inhomogeneous mixing enough explanations? The aim of this work is to answer these important questions. To do so, we have compiled the metal-poor stars from the satellite dwarf galaxies to see if they have the similar pattern. The reason behind this compilation as means of ~~a~~ testing comes from the notion that the CEMP-no stars in the Galactic halo were accreted from their host galaxies, dark-matter dominated low-mass mini-halos. These mini-halos are thought to be disrupted first galaxies, which are analogs of the ultra-faint dwarf (UFD) galaxies (Frebel & Bromm 2012; Salvadori et al. 2016). In this work, we have several exciting results regarding these important questions. Based on the compilation of the satellite galaxy stars described in Section 2, we not only confirm the existence of the multiple CEMP-no groups (Section 4), but also report a discovery of the first CEMP-no Group III stars, SDSS J132755.56+333521.7 (hereafter, SDSSJ1327+3335), in a UFD galaxy, Canes Venatici I (Zucker et al. 2006) in Section 3. Section 4 also reports intriguing results. A subset of Group I CEMP-no stars might have the same origin of Group III CEMP-no stars. Further, the UFDs have both Group II and III CEMP-no stars, whereas the classical dwarf spheroidal galaxies (dSphs) appear to have only Group II CEMP-no stars. Discussion and implications following in Section 4. The summary of our conclusion is following in Section 5.

2. OBSERVATION AND DATA

2.1. *LBT MODS Spectroscopy*

SDSSJ1327+3335 was first identified as a central carbon giant in the discovery paper of CVn I UFD galaxy, by Zucker et al. (2006). There have been spectroscopic follow-up observations (Ibata et al. 2006; Martin et al. 2007; Simon & Geha 2007; Kirby et al. 2010; Vargas et al. 2013; François et al. 2016) for the CVn I galaxy stars but the follow-up of this star has never been done before. We obtained medium-resolution spectroscopy of SDSSJ1327+3335 with Multi-object Double Spectrographs (MODS; Pogge et al. 2010) at the Large Binocular Telescopes (LBT), which have two identical 8.4-meter telescopes. We also observed a canonical ultra metal-poor dwarf carbon star, G 77-61, as a compari-

[2] $A(\mathrm{C}) = \log \epsilon(\mathrm{C}) = \log(N_{\mathrm{C}}/N_{\mathrm{H}}) + 12$, where N_{C} and N_{H} represent number-density fractions of carbon and hydrogen, respectively.

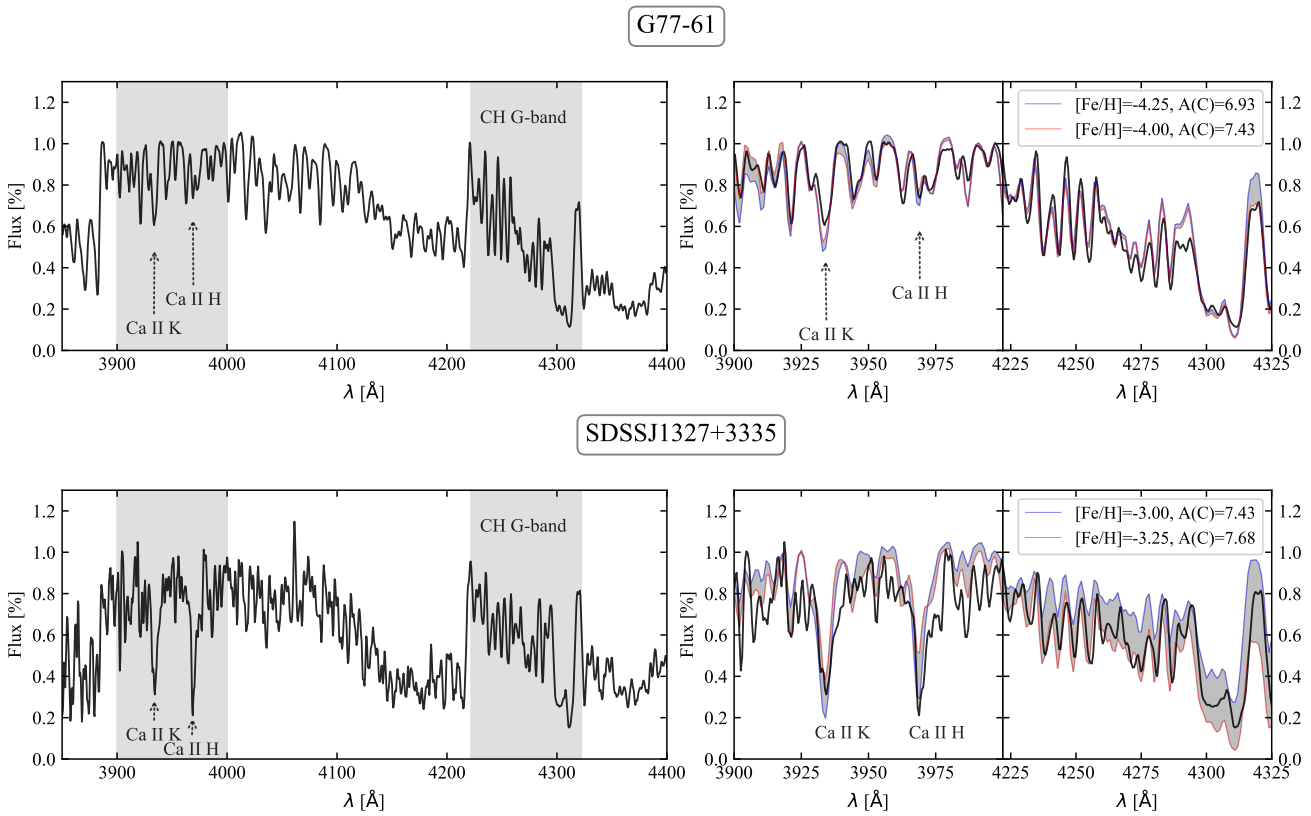

Figure 1. The normalized spectra of G 77-61 (top panels) and SDSS J1327+3335 (bottom panels): The left-side panels represent the observed spectra carried with the LBT MODS. The shaded area represent the wavelength regions of Ca II H, K lines and the CH-band, considered for the reduced χ^2 calculation. The right-side panels show the close-up of the shaded regions on the left-side panels with the synthetic spectra.

son star, whose high resolution stellar parameters are available. Below we provide a description of the observations, data reduction, and a novel method for reliable stellar parameter estimates.

The optical spectra of SDSSJ1327+3335 were obtained on May 21 and June 5 2018. We used the blue grating covering the wavelength range 3200-5800Å, with a dispersion of 0.5 Å pixel^{-1}, which provides a resolution of R $\sim$ 1800. The 0.6 arcsec segmented long-slit was used to obtain eighteen exposures for SDSSJ1327+3335, each with an exposure time of 1200 s. The spectra were flat-fielded, debiased, and bad columns fixed using the modsCCDRed python package[3]. Cosmic rays were identified and removed by using the L.A. Cosmic IRAF[4] task (van Dokkum 2001). The wavelength calibrations were carried out based on observations of Ar lamps on the same run with the standard LBT line lists. Both the wavelength calibration and the one dimensional extraction tasks were carried out using IRAF. Both the MODS 1 and MODS 2 spectra were co-added in the final step. However, three 20-minute exposure MODS2

[3] modsCCDRed by R. W. Pogge, available at http://www.astronomy.ohio-state.edu/MODS/Software/modsCCDRed/

[4] IRAF is distributed by the National Optical Astronomy Observatory, which is operated by the Association of Universities for Research in Astronomy (AURA) under cooperative agreement with the National Science Foundation.

spectra for the June run was not co-added for the final analysis due to a problem with flat spectra. From the co-addition of fifteen spectra (total exposure time 18,000 s), a final signal-to-noise ratio (S/N) of ∼22 per resolution element at 4000 Å was achieved. The spectra of G 77-61 were observed on February 9 2018. For G 77-61, we reduced its spectra with the same procedure as that of SDSSJ1327+3335 except that we used HgAr lamp spectra for the MODS2 data for wavelength calibration. The total exposure time was 3200 s. Its S/N is about 160 per resolution element at 4000 Å.

2.2. *Stellar Atmospheric Parameters*

Due to the presence of ~~very~~ strong CH-band features in a swath of spectra, including Ca II H, K lines for our metallicity estimates, of both SDSS J1327+3335 and G 77-61, the determination of an adequate continuum is ~~very~~ challenging and thus reliable parameter estimates are not straightforward. Here we employ a novel approach to morphological assessment of ~~very~~ cool ($\lesssim$ 4500K), strongly carbon-enhanced stars into the CEMP groups. To do so, we generate archetypal synthetic spectra with [Fe/H] and A(C)~~,~~ best representing the three CEMP groups. For our synthetic spectra, we made use of a grid of model atmospheres computed with the MARCS code (Gustafsson et al. 2008), in which we take the carbon enhancement in the atmosphere into account. We generate synthetic spectra from these model atmospheres using the Turbospectrum routine (Alvarez & Plez 1998), covering the wavelength range of 3000 Å- 10,000 Å. Group I parameters are assumed to be [Fe/H]= −2.5 and A(C)= +7.93, while Group II parameters are [Fe/H]= −3.5 and A(C)= +5.93 and Group III parameters are [Fe/H]=-4.5, A(C)= +7.00. For each of the parameter groups, spectra are generated across the effective temperature range of 4000< $T_{\rm eff}$ (K) < 5500, with surface gravities corresponding to both dwarfs ($\log g$ = 5.0) and giants (0.0 < $\log g$ < 3.5). All synthetic and observed spectra of G77-61 and SDSS J1327+3335 are normalized via the `GISIC` routine[5]. This routine implements a cubic spline interpolation of continuum regions determined from inflection points in the smoothed spectrum. We computed the reduced χ^2 of the spectra for G77-61 and SDSS J1327+3335 as function of temperature (4000 K – 5500 K), corresponding to the region Ca II H, K lines (3900 < λ < 4000) and the CH-band (3922 < λ < 4322) for each CEMP group, for both dwarf and giant types. We verified this synthetic matching technique with G77-61, for which we find that the optimal class is a Group III dwarf star at $T_{\rm eff}$ ∼ 4000 K, which is consistent with the parameters determined from high-resolution spectroscopy (Plez & Cohen 2005). The reduced χ^2 is slightly improved if we adjust the Group III parameters to [Fe/H]=-X.XX and A(C)= $+X.XX$. Using the same procedure for SDSSJ1327+3335, we find the most optimal match to be a Group III giant star at $T_{\rm eff}$ ∼ 4250 K, which is consistent with the photometric $T_{\rm eff}$ from $g-r$ and r, however the fit is improved if we again adjust the Group III parameters to [Fe/H]= $-x.xx$ and A(C)= $+x.xx$. Thus we adopted the best-fit parameters for G 77-61 as [Fe/H] = -x.xx, $T_{\rm eff}$ = 4000 K , log g = 5.0, and A(C) =x.xx, and for SDSS J1327+3335 as [Fe/H] = -x.xx, $T_{\rm eff}$ = 4250 K , log g = x.x, and A(C) =x.xx. The normalized best-fit synthetic spectra along with the observed spectra are shown in Figure 1.

[5] https://pypi.org/project/GISIC/

2.3. *Literature Data Compilation*

We made use of the carbon-normal metal-poor stars from Placco et al. (2014) and the CEMP stars from Yoon et al. (2016) for the Milky Way halo. We updated CEMP stars with carbon detection with recent spectroscopic studies (Aguado et al. 2018; Bonifacio et al. 2018). For the stars from the satellite dwarf galaxies, we used the SAGA database[6] (Suda et al. 2008). The recently observed stars from Tucana II (Chiti et al. 2018) and a CEMP-no star from Pisces III (Spite et al. 2018) were included. We made use of carbon correction calculation[7] (Placco et al. 2014) for restoring carbon abundances of the all samples for consistent comparison. We note that we did not include the halo CEMP-r[8].

I need to check Ani's data for Sculptor

3. SDSSJ1327+3335 IS A CEMP-NO GROUP III STAR

SDSSJ1327+3335 was first identified as a carbon giant in close proximity to the center of the CVn galaxy in its discovery paper by Zucker et al. (2006). There have been spectroscopic follow-up observations (Ibata et al. 2006; Martin et al. 2007; Simon & Geha 2007; Kirby et al. 2010; Vargas et al. 2013; François et al. 2016) for the CVn I galaxy stars but without carbon measurements. In addition, the spectroscopic follow-up of this star was never been reported before. Zucker et al. (2006)

[6] http://sagadatabase.jp

[7] http://vplacco.pythonanywhere.com/

[8] CEMP-r stars are a rarest stellar population among the CEMP stars, whose astrophysical sites have rapid neutron-capture process origin (Ji et al. 2016) and is also thought to be accreted into the halo. Their low A(C) is expected because the CEMP-r stars are not particularly associated with binary system (Hansen et al. 2015)

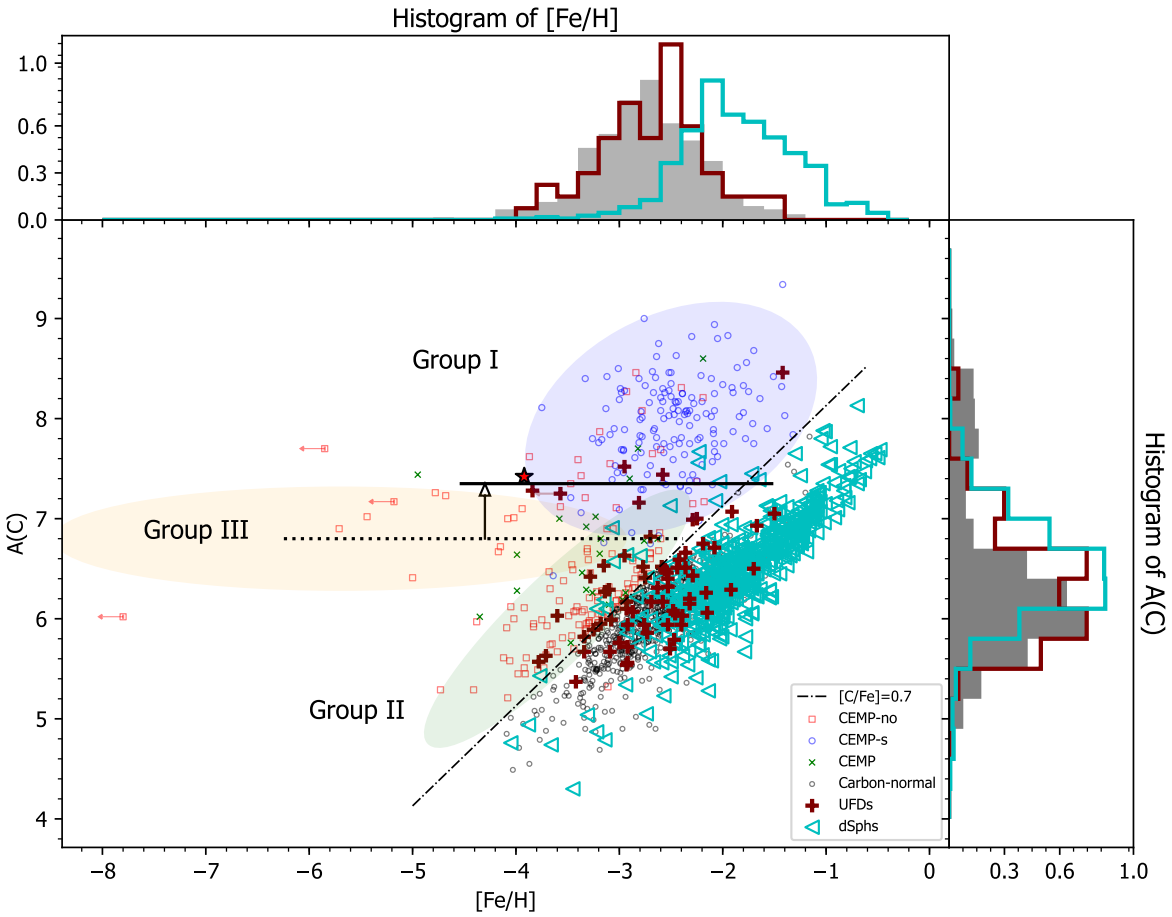

Figure 2. Scatter plot: A distribution of the known CEMP stars in the space of A(C)-[Fe/H]: known dSph (cyan open triangles) and UFDs (maroon '+' signs) along with the halo field stars (CEMP-s/rs stars: blue open circles, CEMP-no stars: red open squares, CEMP stars without Ba detection: green crosses, and carbon-normal stars: gray open circles). Both the gray dotted and solid horizontal lines represent average A(C) levels by eye of the Group III stars in the halo and the satellite galaxies respectively. The top and the right side marginal plots show the histograms of metallicity and A(C) distribution. The filled gray, cyan, and maroon histograms indicate the histograms of the halo, dSph, an UFD stars respectively.

measured the heliocentric radial velocity, 36 ± 20 km/s, of this star and reported its membership to the CVn I. We have checked its parallax and proper motion from the *Gaia* Data Release 2 (Gaia DR2, Gaia Collaboration et al. 2016, 2018; Arenou et al. 2018). However, since it is very faint ($g \sim 20$), both its proper motions and parallax are not reliable due to ~~its~~ low precision. However, its Gaia DR2 parallax is a negative value with a large uncertainty and this indicates that it is unlikely a foreground dwarf star (is that true?). Therefore, we believe this star is a carbon giant member of CVn I. [need to rewrite this paragraph!!!]

Our adopted metallicity ([Fe/H] = -x.xx) and absolute carbon abundance (A(C)= x.xx) assign SDSSJ1327+3335 into CEMP-no Group III. Since other follow-up observations of this galaxy never had carbon abundances, this star makes its first membership of Group III CEMP-no in this galaxy. A follow up of high-resolution spectroscopy will be achieved in the near future. There are known several extremely- and many very metal-poor stars in the CVn I galaxy (Kirby et al. 2010; Vargas et al. 2013) thus we ~~do~~ expect to find more CEMP-no stars in this system once future follow-up of carbon abundances will be soon made.[DO WE NEED MORE HERE FOR SOME IMPLICATIONS?]

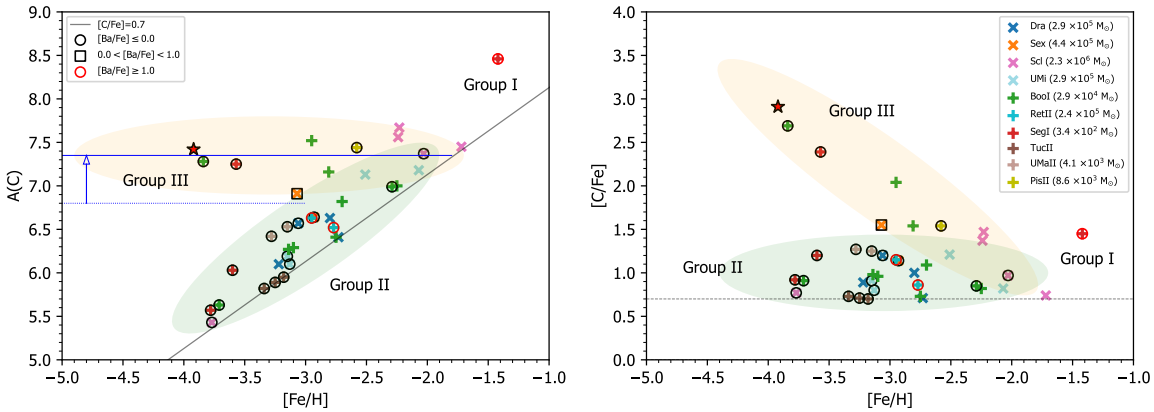

Figure 3. Stellar distribution of the satellite UFDs and dSphs in the spaces of A(C)-[Fe/H] (left panel) and [C/Fe]-[Fe/H] (right panel): The legends in both figures applied to both of the panels. Their host galaxies are indicated in the legend in the right panel. The '+' symbols represent stars from the UFDs and the crosses indicate stars from the dSphs. Symbols in the legend on the left panel (black open circle, black open square, and red open circle) indicate the level of barium enhancement. The gray straight lines in both panels represent the criterion of CEMP stars at [C/Fe]=0.7. The blue dashed and solid horizontal lines in the left panel indicate the average A(C) levels of Group III stars in the halo and the satellite galaxies respectively. The blue arrow indicates the positive carbon abundance shift from the halo stellar distribution to that of dwarf galaxy stars. [I will add another arrow represending the metallicity shift soon.] The name and stellar mass of their host galaxies are found in the legend. [should I get rid of the masses?]

4. THE ORIGIN OF THE CEMP-NO GROUPS : ACCRETION OF SATELLITE GALAXIES

Figure 2 shows the update version of the A(C)-[Fe/H] diagram from Yoon et al. (2016). The new additions are the metal-poor stars from the known satellite galaxies and the carbon-normal stars along with some CEMP stars without Ba detection in the Milky Way halo. The lowest metallicity tail of the metal-poor stars from the dwarf satellite galaxies reaches to [Fe/H]~ -4.0 unlike that ([Fe/H]~ -8.0) of the Milky Way, as shown in the marginal plot of the histogram of [Fe/H] in Figure 2. The higher low metallicity tail of both the UFDs and dSphs is likely from observational limitations due to its faintness and ~~much~~ lower number statistics. In contrast, the higher metallicity tails and mean metallicity of both type of satellite galaxies are drasitically different. The metallicity distribution functions (MDFs) of both the halo stars and the stars from the UFDs are quite similar at [Fe/H]< -2.0 and this similarity indicates an evidence that the Galactic halo formed out of the accretion of the stars from their host mini-halos, as claimed in various studies [reference?]. We note that the MDF in higher metallicity at [Fe/H]> -1.5 in the halo is under-represented due to observational biases. In contrast, the MDF of the dSphs is shifted toward metal-richer regime than that of the UFDs, as ~~clearly~~ seen in the top marginal plot in Figure 2. This shift can be explained in the respect that massive gas reservoir ($(10^3 - 10^4$ more massive than the UFDs) for continuous star formation resulted in higher iron contents in their systems, in turn higher metallicity. On the other hand, the absolute carbon distributions of all three types of galaxies are alike. This may indicate that the cosmic carbon production and its evolution is universal. Therefore, by putting the evolution history of carbon and iron together, we can understand why the dominant stellar population in the dSphs is normal metal-poor stars and only a small fraction ($\sim$2%) of the stars are the CEMP stars. In contrast, a substantial fraction ($\sim$ 28%) of the metal-poor stars from the UFDs are CEMP stars due to ~~its primitive environment likely from~~ truncated star formation due to its small amount of gas available. The contrast in CEMP fractions between the UFDs and the dSphs clearly indicates that the host environment is crucial for understanding the nature of stellar population and influences on the frequency of CEMP stars.

With the environmental factor in mind, we have further inferences based on the morphology of the CEMP stars from the satellite galaxies. Before further discussion, we made a couple of assumptions based on the observation of the behaviors of the CEMP stars from the satellites in Figure 2 and Figure 3. First, the distribution of the satellite galaxy stars is shifted toward higher metallicity (Δ[Fe/H] $\sim +1.0$ dex) and more carbon enhanced (ΔA(C) $\sim +0.6$ dex) than those of the field halo CEMP stars. This shift can be simply understood as the dilution of the metals due to the mixing with the gas available in their host system. Thus the

UFDs and dSphs would have more massive gas to produce more carbon and iron than the already disrupted mini-halos, which deposited their CEMP-no stars into the halo. Secondly, we consider several CEMP stars from the satellite galaxies with higher $A(\mathrm{C}) > 7.1$ and without Ba detection as CEMP-no stars even though those criteria indicate ~~for~~ the division between CEMP-no and CEMP-*s* in the halo. This is because not only the A(C) shift we mentioned above but also we only expect to identify few CEMP-*s* stars in the satellite systems if they exist. The justification behind this expectation is in the similar context to the reason for the lack of CEMP stars in the dSphs. The dSphs have so many iron polluters, which diluted the signature of CEMP, especially in higher metallicity regime ([Fe/H] > -2.0), whose counterpart in the halo are predominantly CEMP-*s* stars. On the other hand, the UFDs do have more primitive, metal-poor stars, mostly [Fe/H] < -2.0 whose analogs in the halo are predominantly CEMP-no stars. The legends of Figure 3, the A(C)-[Fe/H] diagram of the CEMP stars only from the satellite galaxies, show the identification of their host galaxy and the enhancement level of Ba abundance. Fifteen CEMP stars are found in the dSphs (Draco, Sextan, Sculptor, and Ursa Minor) and 22 CEMP stars from the UFDs (Bootis I, Pisces III, Reticulum II, Segue I, Tucana II, and Ursa Major II). As seen in the figure, 15 out of 37 CEMP stars do not have Ba detection. Six out of those 15 stars have $A(\mathrm{C})>7.1$. Three of them are from two dSphs: Sculptor and Ursa Major II with [Fe/H]> -2.5. Other three stars are from the UFDs: Boo I and CVn I. We note that only one CEMP-*s* star with very high $A(\mathrm{C})\sim 8.5$ in Segue I (Frebel et al. 2014) was reported among the satellite galaxies. In addition, two CEMP star from Ret II are CEMP-*r* stars in the sample. [SHOULD I REMOVE THE RET II STARS?] Based on the aforementioned assumptions, we can draw three important inferences.

1. A subset of Group I CEMP-no stars in the halo along the black line of $A(\mathrm{C})= 7.35$ in Figure 2 might have the same origin as that of the Group III CEMP-no stars. Again, we remind that the halo CEMP-no stars in the Group I region have unusually higher A(C) than that of the Group II and III CEMP-no stars. Not all CEMP-no stars in the Group I region can be explained by binary mass-transfer origin. (Yoon et al. 2016).

2. There is a distinct bifurcation into Group II and Group III stars among the CEMP stars from the satellite galaxies, as clearly seen in Figure 2. This is a strong confirmation that the bifurcation of the CEMP-no groups is real in the halo. This similar morphology shown between the halo and the satellite galaxies provides us a strong evidence that the Galactic halo CEMP-no stars were accreted from their host mini-halos.

3. ~~Lastly,~~ only the UFDs have both Groups II and III CEMP-no stars, whereas the dSphs appear to have only Group II CEMP-no stars. If this is valid, this indicate that the Group III CEMP-no stars could be identified only in UFD systems. Since dSphs do have a lot more gas for continuous star formation and show clear chemical evolution in the system, their environment might have diluted the signature of the Group III CEMP-no stars even if they existed. Thus the environment of the least massive systems is the key place to understand the origin of the Group III CEMP-no stars.

Our results, especially, the last inference brings forth a question of the role of the mass of the host galaxies on the bifurcation due to a clear contrast between the masses of the UFDs and the dSphs. In addition, UFDs are dark-matter dominated faint systems and thus have a ~~lot~~ lower stellar mass range compared to that of the dSphs. Dilution of the metals with the gas in the system could play a major role. However, since the UFDs are the most primitive small systems, stochastic star formation and/or local inhomogeneous mixing could influence on the CEMP-no formation as well. In any case, we clearly know that understanding the nature of the CEMP-no stars and its groups relies on knowledge of the masses of their host mini-halos. Further, this can be testable by varying total galaxy mass and the gas-to-dark matter ratio along with stochastic star formation for UFD analogs through the latest cosmological simulations.

5. CONCLUSION

To summarize this work, we have compiled the CEMP stars from the satellite galaxies to compare with the bifurcation of the CEMP-no stars in the halo in the space of A(C)-[Fe/H]. By doing so, we have not only confirmed that two distinct CEMP groups exist in the halo but also in the satellite galaxies. Further, we have discovered a Group III CEMP-no star in the CVn I ultra-faint dwarf galaxy, the first identification of its kind in the system. Based on the similarity of the CEMP group bifurcation between the Milky Way halo and the satellite systems, we provided a strong evidence that the halo formed hierarchically out of numerous accretions of the low mass mini-halos, which are analogs of the UFDs. We also confirm that the UFD systems are the best places to

study the physical and chemical conditions of formation and evolution of the very first stars in the sense that both Group II and Group III stars appear to exist only these faint systems and unlikely developed chemical evolution. The current observational efforts of the CEMP-no stars along with theoretical simulations of galactic chemical evolution and formation will lay the foundation for the future far-field cosmological studies of the first stars through the James Webb Space Telescope and thirty meter-sized ground-based telescopes.

Facilities: Large Binocular Telescopes

J.Y. and T.C.B acknowledge partial support from grant PHY 14-30152; Physics Frontier Center/JINA Center for the Evolution of the Elements (JINA-CEE), awarded by the US National Science Foundation. D.T. participated this work as a REU student at the University of Notre Dame. This paper used data obtained with the LBT MODS spectrographs built with funding from NSF grant AST-9987045 and the NSF Telescope System Instrumentation Program (TSIP), with additional funds from the Ohio Board of Regents and the Ohio State University Office of Research. The LBT is an international collaboration among institutions in the United States, Italy and Germany. LBT Corporation partners are: The University of Arizona on behalf of the Arizona university system; Istituto Nazionale di Astrofisica, Italy; LBT Beteiligungsgesellschaft, Germany, representing the Max-Planck Society, the Astrophysical Institute Potsdam, and Heidelberg University; The Ohio State University, and The Research Corporation, on behalf of The University of Notre Dame, University of Minnesota and University of Virginia. This research made use of NASA's Astrophysics Data System, the SIMBAD astronomical database, operated at CDS, Strasbourg, France, and the SAGA database (Suda et al. 2008; Yamada et al. 2013) (http://sagadatabase.jp). This work has made use of data from the European Space Agency (ESA) mission *Gaia* (https://www.cosmos.esa.int/gaia), processed by the *Gaia* Data Processing and Analysis Consortium (DPAC, https://www.cosmos.esa.int/web/gaia/dpac/consortium). Funding for the DPAC has been provided by national institutions, in particular the institutions participating in the *Gaia* Multilateral Agreement. This work also made extensive use of python.org, astropy (Astropy Collaboration et al. 2013),mplotlib citephunter2007, numpy (Van Der Walt et al. 2011).

Software: astropy (Astropy Collaboration et al. 2013), numpy (Van Der Walt et al. 2011) , mplotlib (Hunter 2007)

REFERENCES

Aguado, D. S., González Hernández, J. I., Allende Prieto, C., & Rebolo, R. 2018, ApJL, 852, L20

Alvarez, R., & Plez, B. 1998, A&A, 330, 1109

Aoki, W., Beers, T. C., Christlieb, N., et al. 2007, ApJ, 655, 492

Arenou, F., Luri, X., Babusiaux, C., et al. 2018, ArXiv e-prints, arXiv:1804.09375

Astropy Collaboration, Robitaille, T. P., Tollerud, E. J., et al. 2013, A&A, 558, A33

Beers, T. C., & Christlieb, N. 2005, ARA&A, 43, 531

Bonifacio, P., Caffau, E., Spite, M., et al. 2018, A&A, 612, A65

Chiaki, G., Tominaga, N., & Nozawa, T. 2017, MNRAS, 472, L115

Chiti, A., Frebel, A., Ji, A. P., et al. 2018, ApJ, 857, 74

Choplin, A., Hirschi, R., Meynet, G., & Ekström, S. 2017, A&A, 607, L3

Clarkson, O., Herwig, F., & Pignatari, M. 2018, MNRAS, 474, L37

François, P., Monaco, L., Bonifacio, P., et al. 2016, A&A, 588, A7

François, P., Caffau, E., Wanajo, S., et al. 2018, ArXiv e-prints, arXiv:1808.09918

Frebel, A., & Bromm, V. 2012, ApJ, 759, 115

Frebel, A., & Norris, J. E. 2015, ArXiv e-prints, arXiv:1501.06921

Frebel, A., Simon, J. D., & Kirby, E. N. 2014, ApJ, 786, 74

Gaia Collaboration, Brown, A. G. A., Vallenari, A., et al. 2018, ArXiv e-prints, arXiv:1804.09365

Gaia Collaboration, Prusti, T., de Bruijne, J. H. J., et al. 2016, A&A, 595, A1

Gustafsson, B., Edvardsson, B., Eriksson, K., et al. 2008, A&A, 486, 951

Hansen, T. T., Andersen, J., Nordström, B., et al. 2016, A&A, 586, A160

—. 2015, A&A, 583, A49

Hunter, J. D. 2007, Computing In Science & Engineering, 9, 90

Ibata, R., Chapman, S., Irwin, M., Lewis, G., & Martin, N. 2006, MNRAS, 373, L70

Ji, A. P., Frebel, A., Chiti, A., & Simon, J. D. 2016, Nature, 531, 610

Kirby, E. N., Guhathakurta, P., Simon, J. D., et al. 2010, ApJS, 191, 352

Lee, Y. S., Beers, T. C., Masseron, T., et al. 2013, AJ, 146, 132

Martin, N. F., Ibata, R. A., Chapman, S. C., Irwin, M., & Lewis, G. F. 2007, MNRAS, 380, 281

Meynet, G., Hirschi, R., Ekstrom, S., et al. 2010, A&A, 521, A30

Nomoto, K., Kobayashi, C., & Tominaga, N. 2013, ARA&A, 51, 457

Placco, V. M., Frebel, A., Beers, T. C., & Stancliffe, R. J. 2014, ApJ, 797, 21

Placco, V. M., Frebel, A., Beers, T. C., et al. 2016, ApJ, 833, 21

Plez, B., & Cohen, J. G. 2005, A&A, 434, 1117

Pogge, R. W., Atwood, B., Brewer, D. F., et al. 2010, in Proc. SPIE, Vol. 7735, Ground-based and Airborne Instrumentation for Astronomy III, 77350A

Salvadori, S., Skúladóttir, Á., & de Bennassuti, M. 2016, Astronomische Nachrichten, 337, 935

Sharma, M., Theuns, T., & Frenk, C. 2018, ArXiv e-prints, arXiv:1805.05342

Simon, J. D., & Geha, M. 2007, ApJ, 670, 313

Spite, M., Spite, F., François, P., et al. 2018, ArXiv e-prints, arXiv:1807.01542

Suda, T., Katsuta, Y., Yamada, S., et al. 2008, PASJ, 60, 1159

Van Der Walt, S., Colbert, S. C., & Varoquaux, G. 2011, ArXiv e-prints, arXiv:1102.1523

Vargas, L. C., Geha, M., Kirby, E. N., & Simon, J. D. 2013, ApJ, 767, 134

Yamada, S., Suda, T., Komiya, Y., Aoki, W., & Fujimoto, M. Y. 2013, MNRAS, 436, 1362

Yoon, J., Beers, T. C., Placco, V. M., et al. 2016, ApJ, 833, 20

Yoon, J., Beers, T. C., Dietz, S., et al. 2018, ApJ, 861, 146

Zucker, D. B., Belokurov, V., Evans, N. W., et al. 2006, ApJL, 650, L41